Adaptive DER and OLTC Control Scheme for Flexible Distribution Grids

Adaptive DER and OLTC Control Scheme for Flexible Distribution Grids

Hannu Laaksonen
School of Technology and Innovations
University of Vaasa
Vaasa, Finland
hannu.laaksonen@uwasa.fi

Nikos Hatziargyriou
School of Electrical and Computer Engineering
National Technical University of Athens
Athens, Greece
nhatziar@mail.ntua.gr

***Abstract*—Flexibility needs of distribution and transmission system operators (DSOs and TSOs) are constantly increasing in renewables-based power systems. In this paper, the TSO-DSO coordinated, adaptive on-load-tap-changers' (OLTCs') and distributed energy resources' (DERs') control scheme for the future flexible distribution grids is further studied and developed. The focus in PSCAD simulation studies with simplified HV/MV/LV network is on cases with two LV feeders which have various types of DERs connected to them with different types of control schemes. This paper studies, for instance, the effect of reactive power (*Q*) -flow-based control of MV and LV battery energy storage systems (BESSs) to minimize upstream reactive power flows as well as compares tan(phi)=-0.35 as reactive power control method for solar photovoltaics (PVs), tan(phi)=-0.35 (discharging) / 0.4 (charging) for BESSs and tan(phi)=0.4 for electric vehicle (EV) chargers to the previously proposed and studied reactive power control principles of DERs. In addition, further improved MV/LV OLTC blocking logic to ensure stable operation is presented.**

***Index Terms*-- Distributed energy resources, Flexible distribution grids, On-load tap changer, Voltage control, Frequency control**

I. INTRODUCTION

Active power (*P*) and *Q* control of the distribution grid-connected DERs with existing grid assets, like OLTCs, offers a very good possibility to fulfill the flexibility needs of the TSOs and DSOs. Flexibility of the DERs can, for example, support the grid voltage (*U*) and frequency (*f*) at the equivalent voltage level. To avoid possible conflict of interest between TSOs and DSOs, improved state-forecasting, monitoring, TSO-DSO coordination and collaborative planning and operation principles for the active utilization of the available flexible energy resources are needed. Therefore, in the future DER units' *Q*- and *P*-control methods and settings should be coordinated with the settings and control principles of the OLTC already in the planning phase. [1]-[3]

In the literature, coordination between DER reactive power-voltage (*QU*)-droop and OLTC settings has been previously examined, for example, in [4] and [5]. This paper studies and develops further the previously presented [6]-[9] adaptive DERs' and OLTCs' control scheme for the future flexible distribution grids in which target is to permit prioritized delivery of flexibility services to the DSOs and TSOs. In this scheme, principles for control of OLTCs' as well as DERs' active power-voltage- (*PU*-), *QU*- and *Pf*-droops will be adapted based on the frequency deviation magnitude level (frequency levels 1-4 are illustrated in Fig. 1). This means that during large frequency deviations (level 4 or 3) TSO's frequency support needs will be prioritized. Respectively, during small frequency differences (level 2 or 1) from the nominal frequency MV/LV and HV/MV OLTCs are planned to be controlled on the basis of the real-time *Q*- and *P*- flows between various voltage levels to improve the DSO grids' DER hosting capacity and to improve the distribution grid-connected DERs' availability for the TSO flexibility services delivery at frequency deviation levels 1-2. In [9], dynamic adaptive and frequency-dependent current/thermal limits utilization for distribution network lines, cables and transformers were also described as part of the overall scheme. [6]-[9]

In this paper, the target is to study by a simple HV/MV/LV grid model cases with two LV feeders which have different types of DERs connected to them with various *P*- and *Q*-control methods together with HV/MV and MV/LV OLTCs' with frequency-dependent management principles. The studies are done with PSCAD simulation software. For instance, the effect of *Q*-flow based control of MV and LV BESSs to minimize upstream reactive power flows are studied as well as tan(phi)=-0.35 as reactive power control method for PVs (French Enedis requirement, [10]), tan(phi)=-0.35 (discharging) / 0.4 (charging) for BESSs and tan(phi)=0.4 for EV chargers are compared to the previously proposed frequency-dependent reactive power control principles of DERs. Also, further improved MV/LV OLTC blocking logic to ensure stable operation is proposed and used in the simulations.

II. STUDY CASES AND SYSTEM

The study system is a simple HV/MV/LV grid (Fig. 1) with rural MV network model including cables, overhead (OH) lines, LV DER units in the 400 V LV grid with two LV

feeders, MV DERs in the middle of the MV feeder as well as OLTCs at MV/LV and HV/MV substations. DER average models that have been used and presented with more details in [6]-[9] and [11]-[16], were used also in this paper. Two MV DER units (1 MW EV charger, 2 MW BESS) and four LV DER units (0.45 MW PV, two 0.2 MW BESSs, 0.2 MW EV charger) are used in the simulations but not necessarily at the same time in each study case (see Tables I-III). In addition, Fig. 1 shows MV/LV and HV/MV OLTCs adaptive control methods, applied adaptive and frequency level-dependent *QU*-/*Q*-, *Q*-flow, *PU*-, and *Pf*- control principles of the DERs as well as the applied behavior of frequency and the changes in the frequency levels over the 250 s simulations during the different study cases (see Tables I-III).

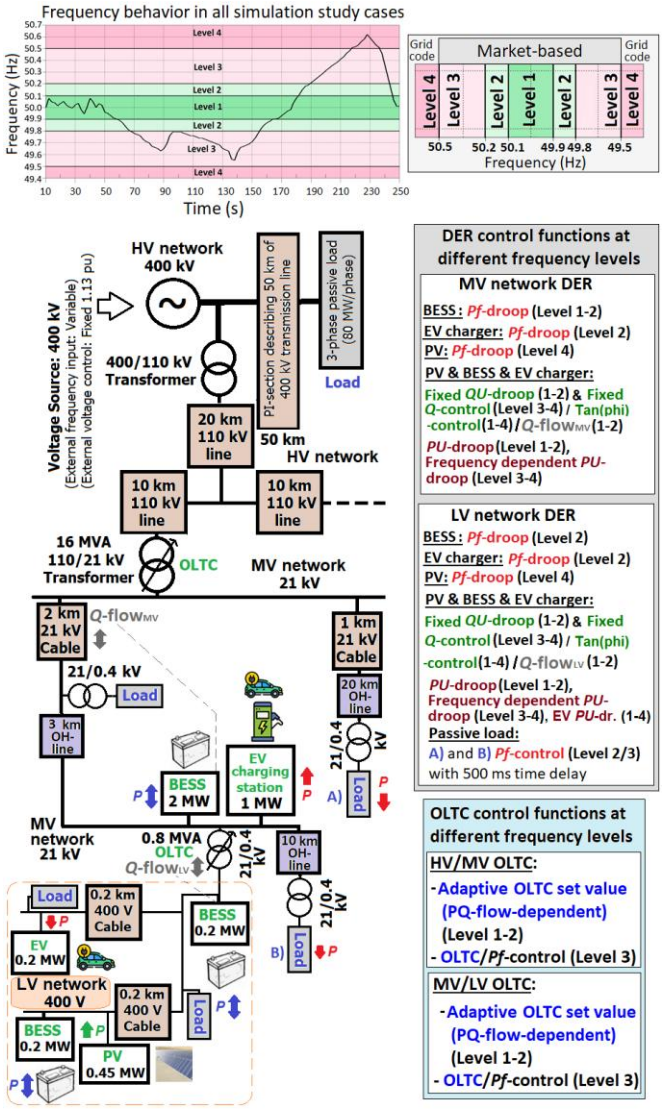

Figure 1. HV/MV/LV network model with MV and LV DERs and their control methods, MV/LV and HV/MV OLTCs and their control principles (see Figs. 2-4) as well as applied behavior of frequency behavior and changes in the frequency levels during the different simulated study cases.

In Fig. 2, OLTC settings which are adapted based on *PQ* flow during the frequency levels 1-2 for MV/LV substation transformers are presented. Adapted OLTC setting based on *PQ* flow during levels 1-2 for HV/MV substation transformers as well as demand response -based MV/LV and HV/MV OLTC settings and operation logic during level 3 are presented in [9] with more details. In Fig. 3, MV and LV DER units' *Pf*-, *QU*-droops, *Q*-flow and *Q*-settings at different frequency levels are shown. Used *PU*-droop settings can be found from [9].

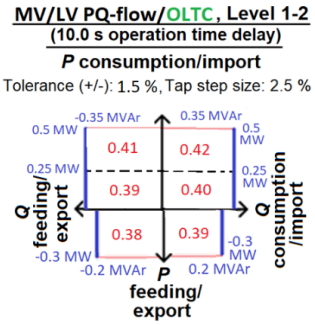

Figure 2. Adaptive OLTC setting based on *PQ* flow for MV / LV substation transformer during levels 1-2, see also Fig. 1).

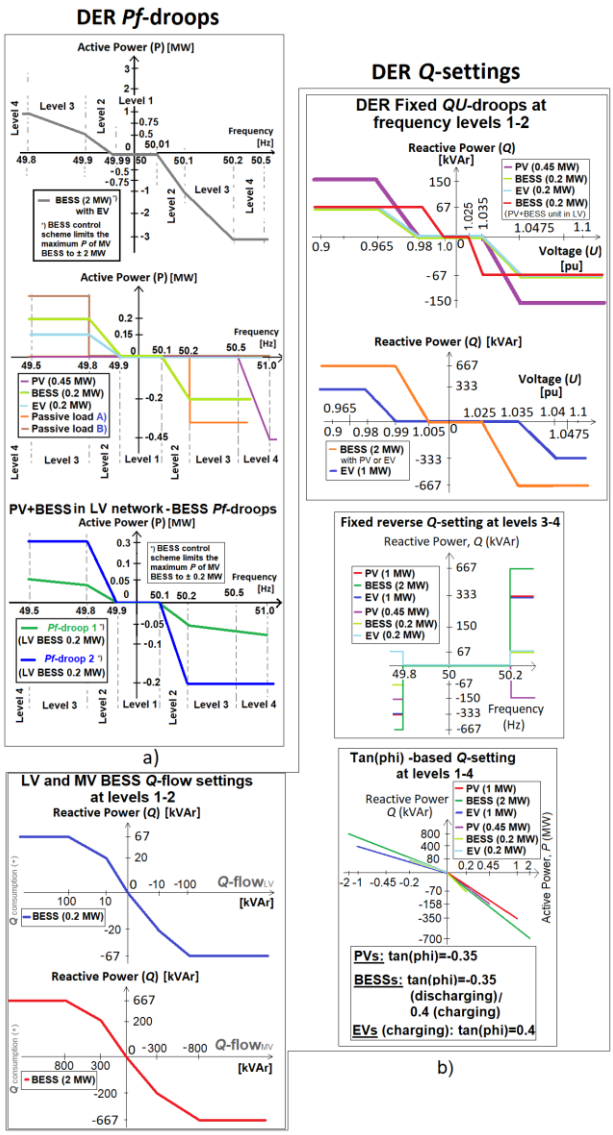

Figure 3. a) LV and MV DERs' *Pf*-droops, b) MV BESS's and LV DERs' *QU*-droops, *Q*-flow or *Q*-settings, see also Figs. 1 and 2).

In this paper, the studied LV network with two LV feeders (Fig. 1) required modification of MV/LV OLTC blocking logic as shown in Fig. 4 when compared to the simulation studies in [6]-[9] to prevent constant ON/OFF operation close to 0.0 MW limit and avoid possible voltage dips due to delayed OLTC control blocking.

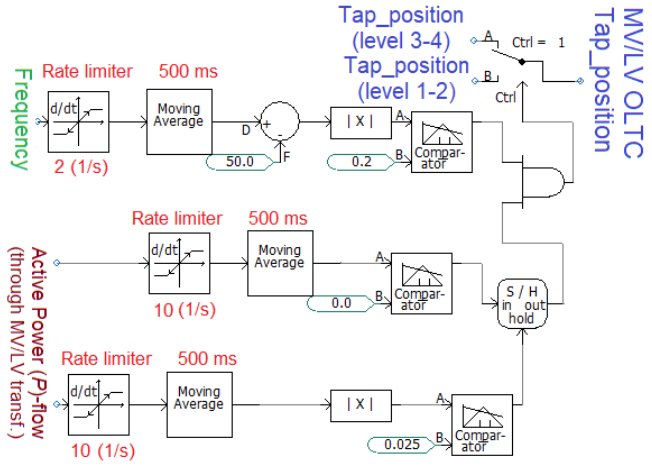

Figure 4. Modified MV/LV OLTC blocking logic (see Fig. 1 and 2).

In Table I, generic information of the studied cases is presented. Table II shows the main study cases CASE 1 and 2 which are used to compare effects of various DER reactive power control methods with a focus on tan(phi)-based control in CASE 2. After that, Table III presents the subcases A-D. When comparing the simulation results in Section III between subcases A-D (Table III) it should be considered that there are different numbers of LV DER units in the studied LV network (highest number of LV DER units in subcase CASE D).

TABLE I
GENERAL INFORMATION ABOUT THE STUDIED CASES (SEE FIGS. 1-4 & TABLES II AND III FOR MORE INFORMATION)

Case*)	Type of MV network	MV DERs' connection point	OLTC control (levels 1-2) / Time delay
All Cases	Rural	Middle of MV feeder	*PQ* flow-based MV / LV) / 10 s & (HV / MV) / 5 s

*) Frequency control settings for demand response (after + / - 0.2 Hz freq. deviation with 500 ms time delay i.e. passive load disconnection/connection at level 2/3, see Fig. 1)

TABLE II
MAIN STUDY CASES WITH DIFFERENT DER REACTIVE POWER (*Q*) -CONTROL SCHEMES (SEE FIGS. 1-4 & TABLES I AND III FOR MORE INFORMATION)

Main Case	MV and LV DERs'	DERs' *Q*-control at level 1-2	DERs' *Q*-control at level 3-4	Adaptation principle of DERs' *Q*-control
CASE 1	MV*): BESS (2 MW), EV (1 MW) LV: 1-2 BESS (0.2 MW), PV (0.45 MW), EV (0.2 MW)	Fixed *QU*-droop / *Q-flow*	Fixed reverse *Q*-setting	Frequency level change (2⇔3)
CASE 2		PVs: tan(phi)=-0.35 BESSs**): tan(phi)=-0.35 (discharging) / 0.4 (charging) EVs (charging): tan(phi)=0.4		-

*) Rapid EV charger (1 MW) at the MV feeder in the same conn. point with MV BESS, more sensitive *QU*-droop with MV BESS (than EV during frequency levels 1-2, MV BESS *P*-control also compensates MV EV's *P* consumption and will supply asymmetrical frequency support, **) In subcase D (Table III) MV and LV BESSs' (at MV/LV substation) with *Q*-flow control at level 1-2

TABLE III
SUBCASES A-D FOR STUDYING EFFECTS OF VARIOUS DER *Q*-CONTROL METHODS (SEE FIGS. 1-4 & TABLES I AND II FOR MORE INFORMATION)

Subcase	LV DERs'	Other Differences
A	BESS (at MV/LV substation), PV, EV	-
B	PV + BESS (in the same conn. point), EV	- PV+BESS: More sensitive *QU*-droop settings with BESS than with PV (CASE 1) and with modified *Pf*-droop 1 (CASE 1 and 2)
C	PV + BESS (in the same conn. point), EV	- PV+BESS: More sensitive *QU*-droop settings with BESS than with PV (CASE 1) and with modified *Pf*-droop 2 (CASE 1 and 2)
D	BESS (at MV/LV substat.), PV + BESS (at the same conn. point), EV	- MV and LV BESSs' (at MV/LV substation) with *Q*-flow control at level 1-2 (CASE 1 and 2) - PV+BESS: More sensitive *QU*-droop settings with BESS than with PV (CASE 1) and with modified *Pf*-droop 2 (CASE 1 and 2)

III. RESULTS OF THE SIMULATIONS

In this section III, the key results of the simulations from the various cases (Tables I-III) are shown. Total time *t* of the simulation in every case was 250 s and applied frequency behavior can be seen from Fig. 1 and Table IV. The PSCAD simulation results from cases of Tables I-III are shown in Figs. 5-7. In Fig. 5, *P* and *Q* flows through the MV/LV and HV/MV substations are presented. Fig. 6 presents the voltages at the end of LV feeders with EV or PV and BESS or only PV as well as at the MV feeder and MV/LV substation. In Fig. 7, A-phase RMS-currents in various cases (Tables I-III) at the beginning of MV feeder (DERs in the middle of the feeder, Fig. 1) as well as through the MV/LV transformer.

TABLE IV
APPLIED CHANGES IN THE FREQUENCY LEVELS DURING SIMULATIONS (SEE FIG. 1)

Time of Level Change	Frequency Level Change
58 s	From frequency level 1 to 2 (1 → 2)
67 s	2 → 3
155 s	3 → 2
165 s	2 → 1
181 s	1 → 2
189 s	2 → 3
217 s	3 → 4
236 s	4 → 3
243 s	3 → 2
245 s	2 → 1

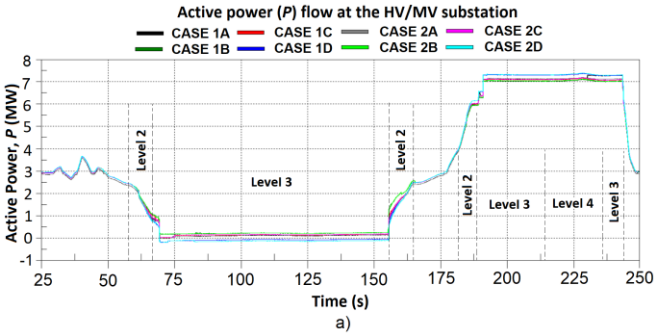

a)

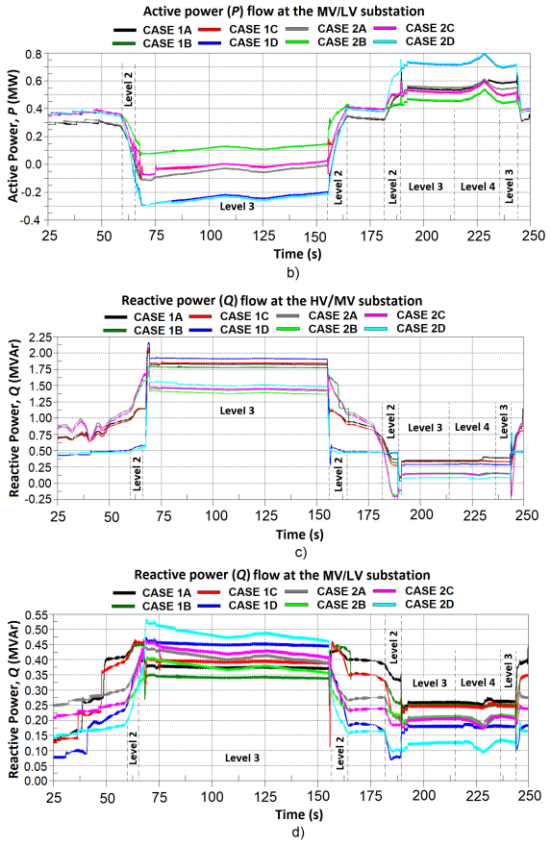

Figure 5. a) *P* flow at the HV/MV subst., b) *P* flow at the MV/LV subst., c) *Q* flow at the HV/MV subst. and d) *Q* flow at the MV/LV subst. in the various cases (see Figs. 1-4 & Tables I-IV).

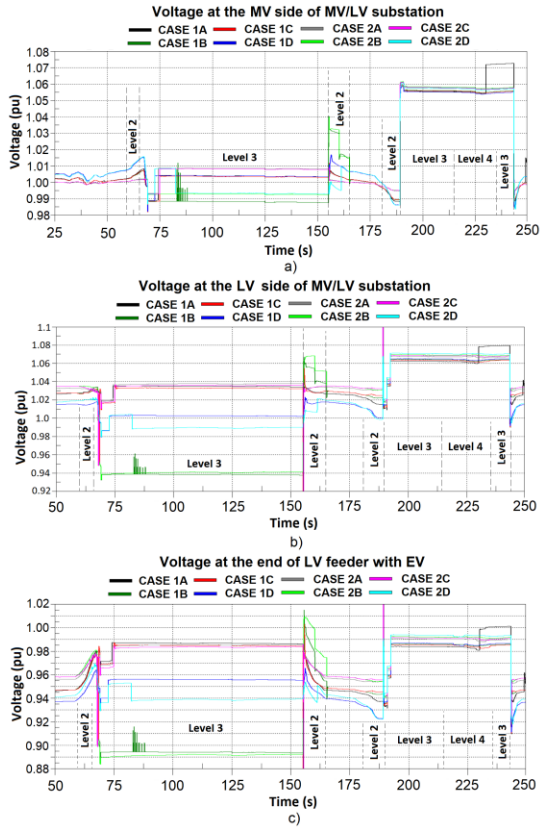

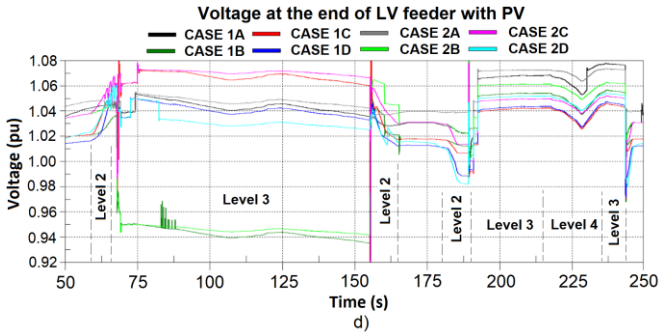

Figure 6. Voltages in various cases at the a) MV feeder i.e. MV side of MV/LV subst. with DERs in the LV network, b) LV side of MV/LV subst., c) end of LV feeder with EV and d) end of LV network feeder with PV+BESS or PV (see Figs. 1-4 & Tables I-IV).

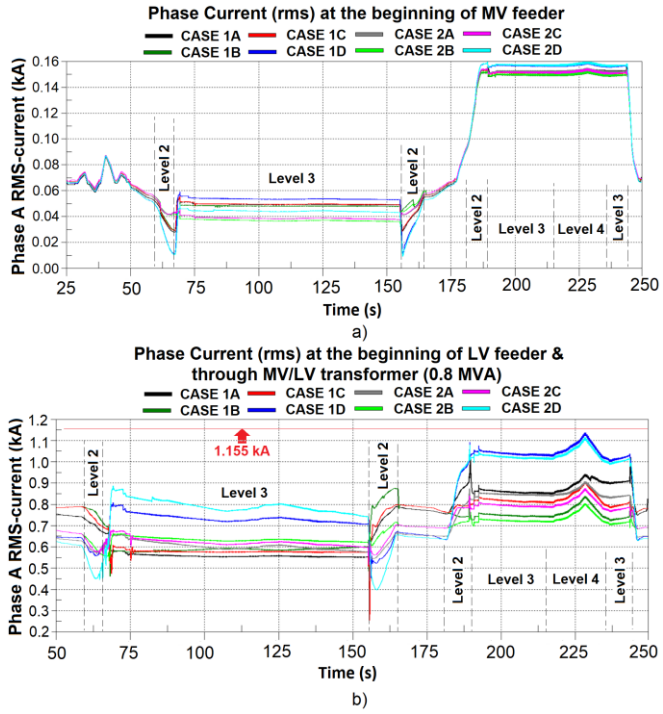

Figure 7. A-phase RMS-currents in various cases a) at the beginning of MV feeder with DERs and b) at the MV/LV transformer's (with DERs in the LV network) LV side (see Figs. 1-4 & Tables I-IV).

One can see from the simulation results (Figs. 5-7), that during more severe level 3 under-frequency situation (at *t*=67-155 s) in the subcases 1B and 2B (Tables II-III), where LV BESSs' had *Pf*-droop 1 (Fig. 3), the *P*-based frequency support (Fig. 5b) was smaller than in the subcases 1C and 2C with *Pf*-droop 2 (Fig. 3). Due to the different LV BESSs' *Pf*-droops in subcases B and C also the *P*-flow through MV/LV transformer (Fig. 5b) was different. Therefore, the MV/LV OLTC blocking logic (Fig. 4) was only activated in subcases C which can be seen as higher LV network voltages during under-frequency (level 3 at *t*=67-155 s) in Figs. 6b)-6d).

From Figs. 5a) and 5b) one can also see that the best *P*-based frequency support during most severe level 3-4 under-frequency (at *t*=67-155 s) and over-frequency (at *t*=189-244 s) was achieved in subcases D (Table III) with one additional 0.2 MW LV BESS at the MV/LV substation (Fig. 1) as well as with MV and LV BESSs' (at MV/LV substation) having

Q-flow-based control at frequency levels 1-2 (Fig. 1, Table III). In CASE 2D with tan(phi)-based DERs' *Q*-control (Table II) the *P*-based frequency support was also a bit higher than in CASE 1D with frequency-dependent *Q*-control (Table II). Simultaneously, during these severe level 3-4 under- and over-frequency situations in CASE 2D *Q*-flow through HV/MV (Fig. 5c) and MV/LV substation was lower than in CASE 1D except through MV/LV substation during under-frequency (level 3 at *t*=67-155 s).

Fig. 5d) shows that generally during level 1-2 frequency deviations the *Q*-flow through MV/LV transformer in subcases (Table III) of CASE 2, with tan(phi)-based DERs' *Q*-control (Table II), is lower than in subcases of CASE 1 (Table II). Simultaneously, the LV network voltages (Figs. 6b-6d) during these level 1-2 frequency deviations are a bit higher in subcases of CASE 2 than in subcases of CASE 1. This is due to the adaptive *PQ* flow -based OLTC settings and control of MV/LV substation transformer during the frequency levels 1-2 (Fig. 2) which are affected by the different DER *Q*-control principles and settings in CASE 1 and 2 (Table II, Fig. 3). One can also see from the simulation results of CASE 1B (Fig. 6) that a similar type of improved OLTC blocking logic (see Fig. 4) would have been needed to avoid too frequent HV/MV OLTC operation during under-frequency (level 3 at *t*=67-155 s).

Q-flow-based control of MV and LV BESS during frequency levels 1-2 in both subcases 1D and 2D also affected quite much to the reactive power flows as shown in Figs. 5c) and 5d) as well as to the simultaneous voltages (see e.g. Figs. 6a and 6b). However, it should be noted that *Q*-flow control through substation transformers or MV feeders requires high-speed low-latency communication from the measurement point/device to the DER unit(s) similarly as in [17] and could simultaneously be used to enable reliable islanding detection with passive islanding detection methods [17]. In addition, feasibility of the communication-based *Q*-flow control can be case-dependent, and the effect of real-time communication delays or disturbances should be further studied in physical tests for both rural and urban grids. Fig. 7b) shows that 0.8 MVA MV/LV transformer's maximum current limit 1.155 kA was not exceeded in the simulations. In addition, 21 kV 4x240 underground cable's max current (I_{max}) limit (0.29-0.375 kA, depends on the installation depth and ambient temperature) was not exceeded at the beginning of MV feeder (Fig. 7a). Further description about the dynamic adaptive and frequency-dependent current/thermal limits for distribution grid lines, cables and transformers can be found from [9].

IV. Conclusions

This paper studied and further developed the adaptive DER and OLTC control scheme for the future active and flexible distribution grids. The PSCAD simulations were done with simple HV/MV/LV grid model, which was modified from the previous studies, for example, so that it included two LV feeders at the LV level and in some of the simulated cases also e.g. the effect of *Q*-flow based control of MV and LV BESSs to minimize upstream *Q*-flows was studied. In addition, tan(phi) as DERs' *Q*-control method was compared to the other *Q*-control principles of MV and LV DERs. Also, further improved MV/LV OLTC blocking logic to ensure stable operation was presented and used in all simulations. In Section III, the key conclusions from the simulations are presented with more details.

Acknowledgments

This study was done as a part of Business Finland funded "Smart Grid 2.0" -project (Grant No. 1386/31/2022).

References

[1] M.-C. Alvarez-Herault et al., "CIRED Working Group - WG 2021-2: Network Planning and System Design with Flexibility," Final Report, ISSN 2684-1088, CIRED 2024.

[2] H. Laaksonen, H. Khajeh, C. Parthasarathy, M. Shafie-khah, and N. Hatziargyriou, "Towards Flexible Distribution Systems: Future Adaptive Management Schemes," *Applied Sciences*, vol. 11, no. 8, 2021.

[3] R. Brazier et al., "TSO – DSO Report, An Integrated Approach to Active System Management with The Focus on TSO – DSO Coordination in Congestion Management and Balancing," report by ENTSO-E, EDSO, EURELECTRIC, CEDEC, GEODE, 2019.

[4] T. Tewari, A. Mohapatra, and S. Anand, "Coordinated Control of OLTC and Energy Storage for Voltage Regulation in Distribution Network With High PV Penetration," *IEEE Transactions on Sust. Energy*, vol. 12, no. 1, 2021.

[5] J. Liu, Y. Li, C. Rehtanz, Y. Cao, X. Qiao, G. Lin, Y. Song, and C. Sun, "An OLTC-inverter coordinated voltage regulation method for distribution network with high penetration of PV generations," *Int. Journ. Electr. Power Energy Syst.*, vol. 113, pp. 991–1001, Dec. 2019.

[6] H. Laaksonen, H. Khajeh, and N. Hatziargyriou, "Advanced Distributed Energy Resources and On-Load Tap-Changer Control Principles for Enhanced Flexibility Services Provision," *IEEE Access*, vol. 12, 2024.

[7] H. Laaksonen, H. Khajeh, and N. Hatziargyriou, "Coordinated Control Schemes for Improved DER Hosting Capacity and Flexibility Provision," in Proc. *CIRED 2024 Workshop*, Vienna, Austria, 2024.

[8] H. Laaksonen, H. Khajeh, and N. Hatziargyriou, "Novel DER and OLTC Management Scheme for Coordinated TSO-DSO Flexibility Services Provision," in Proc. *IEEE PES ISGT Europe 2023*, Grenoble, France, 2023.

[9] H. Laaksonen, and N. Hatziargyriou, "Frequency-dependent Control of DERs and OLTCs in the Future Distribution Networks," in Proc. *CIRED 2025 Conference*, Geneva, Switzerland, 2025.

[10] J. De Lange, S. Rieken, L. Scarabosio, and G. J. Lord, "Preventing Congestion Management by Modelling Cable Temperatures: A Real-World Case," in Proc. *CIRED 2024 Workshop*, Vienna, Austria, 2024.

[11] H. Laaksonen, "Universal Grid-forming Method for Future Power Systems," *IEEE Access*, vol. 10, 2022.

[12] H. Laaksonen, "Improvement of Power System Frequency Stability With Universal Grid-Forming Battery Energy Storages," *IEEE Access*, vol. 11, 2023.

[13] H. Laaksonen, "Solutions to Improve Transient Stability of Universal Grid-forming Inverter-based Resources," *Int. Review of Electrical Engineering (IREE)*, vol. 18, no. 3, 2023.

[14] H. Laaksonen, "Stability of Future Low-Inertia Power Systems with Different Grid-Forming Control Schemes," in Proc. *CIRED 2024 Workshop*, Vienna, Austria, 2024.

[15] H. Laaksonen, and N. Hatziargyriou, "Reconnection of MV Microgrid with Universal Grid-forming Inverter-based Resources," in Proc. *MedPower 2024*, Athens, Greece, 2024.

[16] H. Laaksonen, and N. Hatziargyriou, "Novel DER and OLTC Management During Islanded Operation of MV Microgrid," in Proc. *CIRED 2025 Conference*, Geneva, Switzerland, 2025.

[17] H. Laaksonen, K. Sirviö, S. Aflecht, and P. Hovila, "Multi-Objective Active Network Management Scheme Studied in Sundom Smart Grid with MV and LV Network Connected DER Units," in Proc. *CIRED 2019*, Madrid, Spain, 2019.